AD-A058 621 NATIONAL BUREAU OF STANDARDS WASHINGTON DC SURFACE S--ETC F/G 7/2
THE GEOMETRY OF CO ON RU(001): EVIDENCE FOR BENDING VIBRATIONS --ETC(U)
SEP 78 T E MADEY N00014-78-F-0008
UNCLASSIFIED TR-7 NL

END
DATE FILMED
11-78
DDC

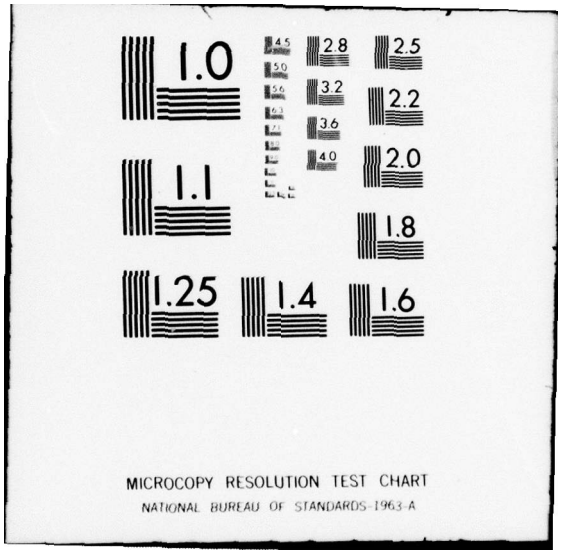
1.0
1.1
1.25
1.4
1.6
1.8
2.0
2.2
2.5
2.8
3.2
3.6
4.0
4.5
5.0
5.6
6.3
MICROCOPY RESOLUTION TEST CHART
NATIONAL BUREAU OF STANDARDS-1963-A

LEVEL II

OFFICE OF NAVAL RESEARCH

Contract N00014-78-F-0008

(15)

(9) TECHNICAL REPORT NO. 7

(12)

(6) THE GEOMETRY OF CO ON Ru(001): EVIDENCE FOR BENDING VIBRATIONS IN ADSORBED MOLECULES

BY

(14) TR-7

(10) Theodore E. Madey

Surface Science Division

National Bureau of Standards

Washington, DC 20234

(11) 1 Sep[redacted]78

(12) 29 p.

To be published in Surface Science

410 655

UNCLASSIFIED

SECURITY CLASSIFICATION OF THIS PAGE (When Data Entered)

REPORT DOCUMENTATION PAGE		READ INSTRUCTIONS BEFORE COMPLETING FORM
1. REPORT NUMBER Technical Report No. 7	2. GOVT ACCESSION NO.	3. RECIPIENT'S CATALOG NUMBER
4. TITLE (and Subtitle) The Geometry of CO on Ru(001): Evidence for Bending Vibrations in Adsorbed Molecules		5. TYPE OF REPORT & PERIOD COVERED Interim 6. PERFORMING ORG. REPORT NUMBER
7. AUTHOR(s) Theodore E. Madey		8. CONTRACT OR GRANT NUMBER(s) N00014-78-0008
9. PERFORMING ORGANIZATION NAME AND ADDRESS Surface Science Division National Bureau of Standards Washington, DC 20234		10. PROGRAM ELEMENT, PROJECT, TASK AREA & WORK UNIT NUMBERS
11. CONTROLLING OFFICE NAME AND ADDRESS Office of Naval Research Physical Program Office Arlington, VA 22217		12. REPORT DATE Sept. 1, 1978 13. NUMBER OF PAGES
14. MONITORING AGENCY NAME & ADDRESS(if different from Controlling Office)		15. SECURITY CLASS. (of this report) Unclassified 15a. DECLASSIFICATION/DOWNGRADING SCHEDULE

16. DISTRIBUTION STATEMENT (of this Report)

Approved for Public Release; Distribution Unlimited.

17. DISTRIBUTION STATEMENT (of the abstract entered in Block 20, if different from Report)

18. SUPPLEMENTARY NOTES

Preprint; to be published in Surface Science.

19. KEY WORDS (Continue on reverse side if necessary and identify by block number)

Surface, adsorption, desorption, electron stimulated desorption, carbon monoxide, ruthenium, bending vibrations.

20. ABSTRACT (Continue on reverse side if necessary and identify by block number)

As a test of the utility of the ESDIAD method (Electron Stimulated Desorption Ion Angular Distributions) in studies of the geometry of adsorbed molecules, the chemisorption of CO on Ru(001) has been examined. Data previously reported using UPS (ultraviolet photoemission spectroscopy) and EELS (electron energy loss spectroscopy) have indicated that CO is terminally bonded to the Ru surface through the C atom, with the CO axis perpendicular to the surface. The ESDIAD results for CO confirm this orientation; for all CO

(Continued on reverse side)

DD FORM 1 JAN 73 1473 EDITION OF 1 NOV 65 IS OBSOLETE
S/N 0102-014-6601

UNCLASSIFIED
SECURITY CLASSIFICATION OF THIS PAGE (When Data Entered)

Block 20 (Continued)

coverages in the temperature range 90 K to ∿ 350 K, the angular distributions of O^+ and CO^+ ESD ions are centered about the surface normal. The widths of the ion beams are temperature dependent; for both O^+ and CO^+, the half widths at half maximum, α, of the ion cones are ∿ 16° at 300 K, and ∿ 12° at 90 K. This temperature dependence, coupled with a simple model calculation indicates that the dominant factors contributing to the width of the ESD ion beams are the CO surface bending vibrations, i.e., initial state effects. Thus, the data suggest that both the directions and widths of ESDIAD beams are determined largely by the structure and dynamics of the initial adsorbed state.

THE GEOMETRY OF CO ON Ru(001): EVIDENCE FOR BENDING VIBRATIONS IN ADSORBED MOLECULES

Theodore E. Madey
Surface Science Division
National Bureau of Standards
Washington, DC 20234

ABSTRACT

As a test of the utility of the ESDIAD method (Electron Stimulated Desorption Ion Angular Distributions) in studies of the geometry of adsorbed molecules, the chemisorption of CO on Ru(001) has been examined. Data previously reported using UPS (ultraviolet photoemission spectroscopy) and EELS (electron energy loss spectroscopy) have indicated that CO is terminally bonded to the Ru surface through the C atom, with the CO axis perpendicular to the surface. The ESDIAD results for CO confirm this orientation; for all CO coverages in the temperature range 90 K to $\sim$ 350 K, the angular distributions of O^+ and CO^+ ESD ions are centered about the surface normal. The widths of the ion beams are temperature dependent; for both O^+ and CO^+, the half widths at half maximum, α, of the ion cones are $\sim$ 16° at 300 K, and $\sim$ 12° at 90 K. This temperature dependence, coupled with a simple model calculation, indicates that the dominant factors contributing to the width of the ESD ion beams are the CO surface bending vibrations, i.e., initial state effects. Thus, the data suggest that both the directions and widths of ESDIAD beams are determined largely by the structure and dynamics of the initial adsorbed state.

I. Introduction

In several recent studies of adsorbed layers on metal surfaces, it has been shown that the ESDIAD method (electron stimulated desorption ion angular distributions) provides detailed insights into surface bonding geometry.[1,2] The directions of emission of positive ions liberated by electron stimulated desorption (ESD) of H_2O, NH_3[3] and C_6H_{12}[4] adsorbed on a Ru(001) surface are consistent with the expected conformation of these surface species. In an effort to further clarify the relationship between surface bond angle and ion desorption angle using ESDIAD, we have studied an adsorption system whose bonding configuration has been reasonably well established, CO on Ru(001).

The adsorption of CO on Ru is of particular interest because of the high activity of Ru as a catalyst for CO hydrogenation to produce methane.[5] The interaction of CO with the Ru(001) surface (the basal plane of hcp Ru) has been characterized using low energy electron diffraction (LEED),[6,7] ultraviolet photoemission spectroscopy (UPS),[8] and x-ray photoemission spectroscopy.[8] Particularly useful structural information has been inferred from the angular resolved UPS studies of Fuggle, Steinkilberg and Menzel[9], and the electron energy loss measurements of Thomas and Weinberg.[10] These latter data indicate that CO is terminally bonded to the Ru(001) surface through the carbon end of the molecule, and is oriented with its molecular axis close to the perpendicular to the surface. This information is also consistent with the known structure of the cluster compound, $Ru_3(CO)_{12}$.[11] Thus, CO on Ru(001) is a nearly ideal test system for the mechanism of the ESDIAD process.

The ESDIAD data reported here are consistent with bonding of the CO molecule perpendicular to the Ru(001) surface. Both CO^+ and O^+ ions are liberated in ESD of adsorbed CO at all coverages, in agreement with recent results of Feulner, Engelhardt and Menzel.[12] The angular distributions of both CO^+ and O^+ ions are centered about the surface normal; the widths at half maximum of the cone angles for ESD of both species are 16° at 300 K. Upon cooling to 90 K, the ion desorption angles decrease to widths at half maximum of 12°. The widths of the ion beams are shown to be consistent with estimates of the amplitudes of bending vibrations of the adsorbed CO. The data suggest that both the direction and widths of ESDIAD beams are determined primarily by the structure and dynamics of the initial state in chemisorption rather than the electronically-excited final state in the ESD process.

Additional results related to the coadsorption of oxygen and CO on Ru(001) are also presented.

II. Experimental

The ultrahigh vacuum apparatus and the experimental procedures employed in these studies have been described previously.[1] The Ru(001) crystal was mounted on an XYZ rotary manipulator and could be resistively heated to 1550 K for cleaning, and cooled to temperatures as low as 90 K for adsorption studies. The surface was cleaned by repeated heating in O_2 followed by heating in vacuo to 1550 K, and the cleanliness of the surface was verified using Auger electron spectroscopy.[7] The sample surface was bombarded by a focussed electron beam ($\sim$ 0.5 mm diam.), and the resultant LEED or ESDIAD patterns were visually displayed using a detector assembly consisting of hemispherical grids and a microchannel plate assembly backed by a fluorescent screen. Mass and angular analysis of the ESDIAD beams were also accomplished by rotating the sample to face a

quadrupole mass spectrometer (QMS) tuned to the mass peak of interest. The axis of rotation was coincident with the sample surface, and the angle between the electron beam and the axis of the QMS was fixed at 38°. This resulted in a variation of the angle of incidence of the electron beam onto the sample of $38° \pm \delta$, where δ was usually $\lesssim 10°$. The symmetry of the experimental ion angular distributions, as well as a simple calculation based on the electron path length in a thin adsorbed layer, indicated that the total ion yield is (to first order) independent of small variations in the angle of incidence. The kinetic energy distribution of an ESD ion beam could be determined using a retarding grid in front of the QMS.

III. Results

A. Mass and Energy Analysis of ESD Ions

The ionic ESD products observed during electron bombardment of CO on Ru(001) were CO^+ and O^+. The dependences of the ESD ion yields as a function of CO exposure are shown in Fig. 1 for the adsorption of CO at $T \sim 300$ K. For these measurements, the axis of the QMS detector was perpendicular to the plane of the sample surface; the focused electron beam (150 eV, 1×10^{-7} A) was used to bombard the crystal intermittently to reduce the possibility of substantial beam-induced damage in the adsorbed layer.[7,12] The CO^+ and O^+ ion signals were of comparable intensity over the entire coverage range, and the functional form of the normalized ion yields in Fig. 1a and 1b are in agreement with the data of Feulner, et al.[12] As shown in Ref. 12 and verified visually in the present study, the maxima in the ion yields coincide with the maximum in the intensity of the $(\sqrt{3} \times \sqrt{3})$ R 30° LEED pattern observed for CO adsorpti . For comparison, the LEED intensity vs. exposure data measured previously[7] are shown in Fig. 1c. The difference in exposure scales is related to ion gauge

calibration differences, etc., in the two measurements. Feulner, et al.[12] concluded that the maxima in the ESD ion yields were due to repulsive CO-CO interactions causing CO to move from sites atop Ru atoms to two-fold bridge sites or three-fold sites at higher coverages. However, the EELS data of Thomas and Weinberg[10] demonstrate that CO bonding is substantially the same from low to high coverage. There is no large vibrational shift which would occur if the CO changed its state of hybridization in going from atop to bridge sites; a model based on two types of CO bonding at low and high coverages is not supported by these data.[10] The disordering of the CO layer at $T \gtrsim 300$ K[7], the out-of-registry LEED patterns at $T \sim 100$ K[13], and the reduction of CO^+ and O^+ ion yields at high coverage are apparently a result of more subtle bonding changes (e.g., out-of-registry displacements due to lateral interactions) than movement to multiply coordinated high symmetry sites.

The observation of CO^+ and O^+ ions and the absence of C^+ ions is evidence that the CO molecules are bonded via the carbon atom (in gas phase dissociative ionization of CO, the C^+ yield is greater than the O^+ yield).[14]

Retarding potential plots, uncorrected for work function differences, are shown in Fig. 2 for the ESD of CO^+ and O^+. These data correspond to a CO exposure of 1.5L, at the maximum ion yield (i.e., at ~ 0.5 of the saturation CO coverage). The kinetic energy difference of ~ 5 eV between O^+ and CO^+, as well as the observation of higher kinetic energies for the O^+ ions, has been observed previously in ESD studies of CO on W.[15-17] Correcting for work function differences, the most probable CO^+ kinetic energy is ~ 2 eV, and the most probable O^+ kinetic energy is ~ 7 eV. These retarding potential results are independent of CO coverage ($\theta = 0.5$ and 1.0), sample temperature (adsorb at 300 K; measure at 300 K or at 90 K) and electron bombardment energy (130 eV to 170 eV). Only when the CO is adsorbed on a partially-oxygen covered surface

were differences observed: the difference between the O^+ and CO^+ kinetic energies increased to $\sim$ 6.3 eV, as the CO^+ kinetic energy decreased by $\sim$ 1 eV.

B. Angular Distributions of ESD Ions

Visual examination of the ESDIAD patterns for CO on Ru(001) revealed that the CO^+ and O^+ ions desorb in a narrow cone of emission normal to the surface. At all CO coverages, and for adsorption temperatures in the range 90K to $\gtrsim$ 300K, the only ESDIAD patterns observed were indicative of ion desorption perpendicular to the surface; no off-normal beams were seen. The "central spot" in the ESDIAD patterns appeared to be circular, with no evidence of azimuthal anisotropy. The results are in qualitative agreement with the ESDIAD data for CO on W(111).[18] Thus, the directions of CO^+ and O^+ desorption are consistent with the angular resolved UPS and the EELS evidence for terminal bonding of CO to Ru(001), with the CO axis perpendicular to the surface.

We now address the questions: what are the angular widths of the ion beams, and what are the physical factors which influence the ion beam widths? In particular, is there any temperature dependence of the beam widths which can be quantitatively related to the bending vibrational amplitudes of the adsorbed CO? In an earlier ESDIAD study of oxygen on W(100)[19], a reversible temperature dependence in ion beam size was observed and related to surface vibrations.

Angular distributions for CO^+ and O^+ were measured by rotating the crystal to face the QMS and measuring the QMS ion signal as a function of ion desorption angle. Two typical angular distributions are shown in Fig. 3; in each of these cases, the CO was dosed onto the crystal at 300K and cooled to 90K for the measurements. For each angular distribution measurement, the crystal was biased positively by a potential V_B with respect to the (grounded) retarding grid at the entrance to the QMS. This was necessary in order to

maintain an adequate signal-to-noise ratio and to overcome the influence of weak stray fields. The half width at half maximum (hwhm) of each angular distribution is defined as the cone angle α ; the value of α for O^+ is greater than α for CO^+ in these measurements. As will be discussed below, one effect of the bias potential is to deflect the ion trajectories and decrease the measured value of α below the true value, α_o. Because the O^+ ions have

considerably higher initial kinetic energies than the CO^+ ions, the distortion of the O^+ trajectories is less than that of the CO^+.

In order to provide a zeroth order correction to the angular distribution data for the distorting influence of the electric field arising from the bias potential, classical trajectory calculations were performed. Assuming that the electric field could be represented by a plane parallel field, values of α as a function of V_B were computed, with ion mass, ion kinetic energy, and true desorption angle α_o as parameters.

Figure 4 contains plots of α vs V_B measured under different conditions. In each case, the Ru(001) crystal was dosed with 1.5L of CO at $\sim$300 K; measurements were made either at 300 K or after cooling the sample to 90 K. Each data point corresponds to a value of the cone angle α given by the hwhm of an ion angular distribution similar to those of Fig. 3. The top panel shows data for O^+ at 300 K and 90 K; the bottom panel shows corresponding data for ESD of CO^+. In each case, the solid line is a visual fit to the experimental data based on the classical trajectory calculation; the parameters used in each calculation are indicated on the figure. A purpose of the figure is to demonstrate the method used for determination of the zero field or true cone angle α_o, as well as the temperature dependence of α_o. Based on the extrapolation shown, for both O^+ and CO^+ at 300 K, $\alpha_o \simeq 16°$; for both O^+ and CO^+ at 90 K, $\alpha_o \simeq 12°$.

Based on uncertainties in the measurements of E_{kin} and of α, the estimated uncertainty of α_o is $\pm$ 1° for O^+ and $\pm$ 3° for CO^+ (within the framework of the trajectory calculation). The magnitudes of the systematic contributions to the errors in determination in α_o, due to deviations from the assumed functional form of the electric field in the trajectory calculations, are not known. It

is worth noting, however, that the higher the initial ion kinetic energy, the less important is the mathematical form of the correction. Even linear extrapolations of the O^+ data of Fig. 4a yield values of α_o within 2° of the corrected values.

Measurements similar to those of Fig. 4 were also made for a saturation CO coverage ($\sim$ 5 L) on the Ru(001) surface at 300 K. The data are best fit by $\alpha_o = 15°$ for O^+ and $\alpha_o = 16°$ for CO^+, but the experimental uncertainties are greater than this difference. Based on the higher accuracy of the O^+ measurements, we suggest that α_o is approximately equal to 15° for both O^+ and CO^+ at high CO coverage at 300 K. Thus, the CO-CO repulsive interaction which causes the surface layer to disorder at high coverages at 300 K may also cause a small reduction in the width of the ESD ion angular distributions.

C. Coadsorption of CO and O

Davydov and Bell[20] have recently used infrared spectroscopy to study the adsorption of CO on a silica supported Ru catalyst. They observed that when the Ru is covered with oxygen, a pair of infrared bands whose intensities are correlated suggest that there are two CO molecules adsorbed at each site, as shown below.

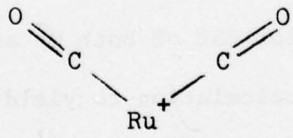

In an effort to see whether or not such a structure forms on the Ru(001) plane, we have used ESDIAD to study CO adsorption on the oxygen covered surface. Various coverages of both CO and oxygen were studied under the following conditions: (a) CO was adsorbed both at 300 K and at 90 K onto

the ordered, saturated oxygen covered surface characterized by the (2 x 2) LEED pattern,[21] and (b) CO was adsorbed at 90 K onto the disordered oxygen-covered surface prepared by adsorption of oxygen at 90 K.[21] In all cases, the ESDIAD pattern associated with the coadsorption of CO and oxygen was characterized by a central spot, i.e., coincident O^+ and CO^+ beams desorbing normal to the surface. The results are clearly consistent with terminal CO bonding perpendicular to the surface, with no evidence for the structure reported by Davydov and Bell. We conclude that this structure does not form on the Ru(001) surface; perhaps rougher, more open surfaces are necessary to stabilize this complex.

A series of measurements of ion angular distributions, analagous to those of Fig. 3 and 4, were made for CO adsorbed onto the ordered (2 x 2) oxygen covered Ru surface at 300 K. (This surface was prepared by dosing the clean Ru surface at 300 K with an O_2 exposure of 10 L, followed by heating to 900 K for $\sim$ 1 sec). The CO coverage in each case was produced by a 1.5 L dose of CO and was judged using temperature programmed desorption to be nearly identical to that of Fig. 3 and 4. The data plotted in Fig. 5 as α vs V_B for ESD of both O^+ and CO^+, can be fit using the classical trajectory calculation to yield a value of $\alpha_o = 15°$ for both O^+ and CO^+. Thus, the value of α_o is slightly less than that observed for the corresponding CO coverage on the oxygen free surface.

IV Discussion

The observation of CO terminally bonded through the C atom perpendicular to the surface of a transition metal is in agreement with many other bits of evidence. The MCO bond in terminally bonded transition metal carbonyls is usually linear and the small deviations from linearity ($\sim 7°$) reported[11] in $Ru_3(CO)_{12}$ may be a result of thermal vibrations and experimental uncertainty. The angular resolved UPS data of Allyn and Plummer[22] for CO on Ni(100) indicate that CO "stands up" on this surface. Recently, however, there have been at least two reports of "tilted" CO. Anderson and Pendry[23] report that CO on Ni(100) is inclined by $34° \pm 10°$ away from the normal, and Rhodin[24] has reported evidence for tilted CO on Ir(111). The advantage that ESDIAD offers over the complex LEED analysis is its directness: one can literally see the directions of ion emission, and by implication, the surface bond directions. This conclusion is supported both by experimental observations[1,3] and the recent calculations of Clinton.[25]

Clinton[26] has argued, consistent with the temperature dependence reported earlier[18] that vibrational as well as structural information may be available in ESDIAD. Gersten et al.[27] have also presented theoretical evidence for the role of surface vibrations in ESDIAD. Clearly, the observation of a strong temperature dependence in the cone angle α_o for ESDIAD of CO implies that bending vibrational modes in the initial state play a major role in determining ion desorption angles. The question we wish to address now is: what are the respective contributions of initial and final states to the angular width of an ion angular distribution?

We first consider the influence of final state effects on the ion trajectories. The final state effects which can cause broadening of the ion beams include the angular anisotropy of ion neutralization, the "defocussing" because of curvature in the repulsive final state potential, and the image force acting on the desorbing ion. In the absence of detailed knowledge of the final state force field and the parameters influencing the anisotropy of ion neutralization, the first two factors cannot easily be estimated. We can, however, estimate the influence of the image potential on the ion trajectories. Clinton[25] has shown that an ion desorbing with an initial angle α_i with respect to the surface normal will arrive at the detector with an apparent desorption angle α_o given by

$$\cos \alpha_o = \cos \alpha_i \left[\frac{1 + V_I/(E_K - V_I)\cos^2 \alpha_i}{1 + V_I/(E_K - V_I)} \right]^{1/2} \qquad (1)$$

V_I is the (screened) image potential[28] at the initial ion-surface distance Z_o, and E_K is the measured kinetic energy of the desorbing ion. Note that V_I is a negative quantity, $\left| V_I/(E_K - V_I) \right|$ is ≤ 1, and $\alpha_o \geq \alpha_i$. Thus, the effect of the image potential is to systematically increase the measured desorption angle α_o over the initial desorption angle α_i. Inserting values appropriate to the desorption of O^+ from CO on Ru(001) (V_I = -1.52 eV, E_K = 7 eV, Z_o = 1.9 Å), eq. 1 predicts that $\alpha_i = 14.5°$ when $\alpha_o = 16°$, and $\alpha_i = 10.8°$ when $\alpha_o = 12°$.

For CO^+, the correction is even larger due to its smaller value of E_K. Using V_I = -1.9 eV, E_K = 2 eV, Z_o = 1.32 Å, eq. 1 predicts that $\alpha_i = 11.4°$ when $\alpha_o = 16°$, and $\alpha_i = 8.5°$ when $\alpha_i = 12°$.

Since the experimental uncertainty in α_o and the magnitude of the image correction is much smaller for O^+ than CO^+, we shall confine our further remarks to the case of O^+. Specifically, we shall show that after correcting

for the image potential effect, the balance of the ESDIAD O^+ beam width can be explained almost entirely on the basis of initial state effects, viz., the amplitude of surface vibrational modes about the surface normal.

In examining the vibrational contributions to α_i, only bending vibrations will be considered, since stretching modes of CO or RuCO will not (to a first approximation) influence α_i. The low frequency infrared and Raman data of Quicksall and Spiro[29] for $Ru_3(CO)_{12}$ have been used to estimate the force constants and vibrational frequencies for adsorbed CO on Ru(001). We assume that the Ru-C-O bending motions are characterized by two types of vibrations in which the Ru lattice is assumed to be essentially rigid:

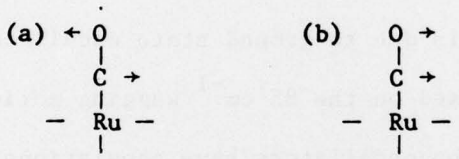

The two degenerate bending modes (a), characterized by vibrations in orthogonal directions, are approximated by the carbonyl Ru CO bending vibrations having vibrational frequencies in the range 500 cm^{-1} to 600 cm^{-1}; for the following calculation, the average frequency of 550 cm^{-1} is chosen, along with the valence force constant k_B = 0.90 mdyn Å x rad^{-2} [29]. The degenerate wagging modes (b) are approximated by the carbonyl C-Ru-C bending vibrations which have prominent Raman bands at 125, 85, and 47 cm^{-1}. For the following calculation, the values 85 cm^{-1} and k_B = 0.26 mdyn Å x rad^{-2} are used.[29]

The simplest estimate of the angular vibrational amplitude is given by the classical approximation for torsional simple harmonic motion,

$$E_n = (n + 1/2)\, h\nu \approx 1/2\, k_B\, \theta_n^2 \qquad (2)$$

where E_n is the vibrational energy, n is the vibrational quantum number (0,1,2 ...), h is Planck's constant, ν is the vibrational frequency in sec^{-1},

k_B is the bending force constant, and θ_n is the classical limiting angular vibrational amplitude, in radians, for the oscillator in the n^{th} vibrational state. The relative populations of the different vibrational levels (relative to the n = 0 ground state level) is given by the Boltzman expression

$$\frac{N_n}{N_o} = \exp\left\{-\frac{nh\nu}{kT}\right\} \tag{3}$$

Values of θ_n (expressed in degrees) and N_n/N_o (based on eq. (2) and (3) and the appropriate values of ν and k_B) are tabulated in Table I. It is apparent from these results that the major contribution to the temperature dependence of the CO bending amplitude is the 85 cm^{-1} bend. Even at 300 K, most of the 550 cm^{-1} bending amplitude is due to ground state oscillators (θ = 6.3°). In choosing values of θ_n based on the 85 cm^{-1} wagging motion to compare with the ESDIAD data, we note that the oscillators have populations $\gtrsim$ 0.25 of the maximum (ground state) population for vibrational amplitudes of 8° (90K) and 12.2° (300K).

We now estimate the initial state contribution to the width of the O^+ ion beam $\alpha_{IS}(T)$ by a statistical sum of vibrational and instrumental contributions. Assuming that the various terms can be represented by Gaussians, the angular hwhm's can be expressed as

$$\alpha_{IS}^2(T) = \theta_i^2(85\ cm^{-1}) + \theta_j^2(550\ cm^{-1}) + \alpha_{res}^2 \tag{4}$$

Here, $\alpha_{IS}(T)$ is a function of temperature T, as are $\theta_i(85\ cm^{-1})$ and $\theta_j(550\ cm^{-1})$. The quantity α_{res} is the instrumental resolution, determined to be 2° from the geometry of the limiting apertures. From Table I, we estimate that at 90K, $\theta(85\ cm^{-1}) \simeq 8.0°$ and $\theta(550\ cm^{-1}) \simeq 6.3°$; at 300K, $\theta(85\ cm^{-1}) \simeq 12.2°$ and $\theta(550\ cm^{-1}) \simeq 6.3°$. Using these numbers in eq. (4), we get

$$\alpha_{IS}(90K) = 10.4°$$

and $$\alpha_{IS}(300K) = 13.9°.$$

These numbers are to be compared with the experimental values of the hwhm of the O^+ ion beams which have been corrected for the image potential using Eq. (1), i.e., $\alpha_i(90K) = 10.8°$

and $\alpha_i(300K) = 14.5°$.

These data are summarized in Table II. Within the framework of the simplifying assumptions, it appears that a substantial fraction of the broadening of the ESD ion beams is due largely to the initial state bending vibrations.

The above calculation was simply intended to demonstrate the order of magnitude of vibrational effects; in view of the simplifying assumptions, the remarkable agreement between theory and experiment is certainly fortuitous. We do not know the exact bending frequencies and valence force constants for CO on Ru(001), and they may be different from those of $Ru_3(CO)_{12}$ used here. The bending frequencies[30,31] for $W(CO)_6$, $Mo(CO)_6$, $Cr(CO)_6$, and $Ni(CO)_4$ are all similar to those of $Ru_3(CO)_{12}$, but there is a considerable range of bending force constants reported. From Eq. (2), the use of higher force constants would result in smaller values of θ_n and α_{IS}. Ideally, if better force constants and bending frequencies for CO on Ru(001) were known, a normal coordinate treatment of the Ru-C-O system would be necessary to compute the bending amplitude accurately. Since these data are not available, this was not attempted. Finally, the temperature dependence of substrate Ru atom motion (i.e., the Debye-Waller effect) is expected to be small in comparison with the CO bending amplitudes.

We note in closing that Niehus[32] has recently examined the ESDIAD of CO^+ and O^+ from α-CO on W(111) at 300 K. The ions desorb in a cone normal to the surface, with fwhm $\sim$ 16°, in good agreement with the present results for Ru(001).

V. Conclusions

The ESDIAD data for CO on Ru(001) are consistent with a bonding model in which CO is bonded perpendicular to the Ru surface. Furthermore, the temperature dependence of the ESDIAD beam widths are consistent with estimates of the bending vibrations of adsorbed CO. The width of an ESDIAD beam at temperature T reflects a "snapshot" of the statistical distribution of atom (molecule) positions with respect to the equilibrium position at that temperature. The data indicate that both the ion desorption directions and the widths of the ion beams are determined largely by intial state effects, i.e., the structure and vibrational dynamics of the adsorbed species.

VI. Acknowledgements

The author acknowledges with pleasure valuable discussions with Dr. Glenn Thomas (Caltech), Dr. A. M. Bradshaw, Dr. H. Niehus, Dr. W. J. Lafferty, Dr. S. Abramowitz, and Dr. W. L. Clinton as well as a critical reading of the manuscript by Dr. J. T. Yates, Jr. Dr. K. Revesz assisted with a computer calculation, and Ms. Maureen Madey assisted with data analysis. This work was supported in part by the Office of Naval Research.

REFERENCES

(1) T. E. Madey and J. T. Yates, Jr., Surface Science 63, 203, 1977; J. J. Czyzewski, T. E. Madey and J. T. Yates, Jr., Phys. Rev. Lett. 32, 777 (1974).

(2) H. Niehus, in R. L. Dobrozemsky, ed., Proc. 7th Intern. Vac. Cong. and 3rd Intern. Conf. Solid Surfaces, Vienna 1977 (R. Dobrozemsky, et. al., Publ.) p. 2051.

(3) T. E. Madey and J. T. Yates, Jr., Chem. Phys. Lett. 51, 77 (1977); T. E. Madey and J. T. Yates, Jr. in R. L. Dobrozemsky, ed., Proc. 7th Intern. Vac. Congr. and 3rd Intern. Conf. Solid Surfaces, Vienna, 1977 (R. Dobrozemsky et al., publ.) p. 1183.

(4) T. E. Madey and J. T. Yates, Jr., Surface Science, to be published.

(5) M. A. Vannice, Catal. Rev.-Sci. Eng. 14, 153 (1976).

(6) J. T. Grant and T. W. Haas, Surface Science 21, 76 (1970).

(7) T. E. Madey and D. Menzel, Japan. J. Appl. Phys., Suppl. 2, Pt. 2, 229 (1974).

(8) J. C. Fuggle, T. E. Madey, M. Steinkilberg and D. Menzel, Surface Science 52, 521 (1975).

(9) J. C. Fuggle, M. Steinkilberg and D. Menzel, Chem. Phys. 11, 307 (1975).

(10) G. E. Thomas and W. H. Weinberg, Nederlands Tijdschrift voor Vacuumtechniek 16, 57 (1978).

(11) R. Mason and A.I.M. Rae, J. Chem. Soc. (A), 778 (1968).

(12) P. Feulner, H. A. Engelhardt, and D. Menzel, Appl. Phys. 15, 355 (1978).

(13) E. Williams and W. H. Weinberg, private communication.

(14) American Petroleum Institute Project 44, Mass Spectral Data (1960).

(15) D. Menzel, Ber. Bunsenges. Physik. Chem. 72, 591 (1968).

(16) M. Nishijima and F. M. Propst, J. Vac. Sci. Technol. 7, 420 (1970).

(17) J. T. Yates, Jr. and D. A. King, Surface Science 32, 479 (1972).

(18) T. E. Madey, J. T. Czyzewski, and J. T. Yates, Jr., Surface Science 57, 580 (1976).

(19) T. E. Madey, J. J. Czyzewski, and J. T. Yates, Jr., Surface Science 49, 465 (1975).

(20) A. A. Davydov and A. T. Bell, J. Catalysis 49, 332 (1977).

(21) T. E. Madey, H. A. Engelhardt, and D. Menzel, Surface Science 48, 304 (1975).

(22) C. L. Allyn, in R. L. Dobrozemsky ed., Proc. 7th Intern. Vac. Congr. and 3rd Intern. Conf. Solid Surfaces, Vienna, 1977 (R. Dobrozemsky et al., publ.) p. 497; E. W. Plummer, ibid. p. 647.

(23) S. Andersson and J. B. Pendry, Surface Science 71, 75 (1978).

(24) T. N. Rhodin, C. Brucker, J. Kanski, C. Seabury, G. Broden, Z. Hurych and R. Benbow, Bull. Am. Phys. Soc. 22, 415 (1977).

(25) W. L. Clinton, to be published.

(26) W. L. Clinton, Phys. Rev. Letters 39, 965 (1977).

(27) J. I. Gersten, R. Janow and N. Tzoar, Phys. Rev. Lett. 36, 610 (1976).

(28) J. W. Gadzuk, Surface Science 67, 77 (1977).

(29) C. O. Quicksall and T. G. Spiro, Inorg. Chem. 7, 2365 (1968).

(30) L. H. Jones, R. S. McDowell and M. Goldblatt, J. Chem. Phys. 48, 2663 (1968).

(31) L. H. Jones "Inorganic Vibrational Spectroscopy" (Dekker, New York, 1971).

(32) H. Niehus, private communication.

TABLE I

Calculations of Vibrational Characteristics of CO on Ru(001)

(a) Bending modes, 550 cm^{-1} $\quad k_B = 0.90$ mdyn x A x rad^{-2}

n	θ_n	N_n/N_o (90K)	N_n/N_o (300K)
0	6.3°	1	1
1	10.9°	1.5×10^{-4}	0.072
2	14.1°	1.4×10^{-8}	0.0044

(b) Wagging modes, 85 cm^{-1} $\quad k_B = 0.26$ mdyn x A x rad^{-2}

n	θ_n	N_n/N_o (90K)	N_n/N_o (300K)
0	4.6	1.0	1.0
1	8.0	.26	.67
2	10.3	.066	.44
3	12.2	.017	.29
4	13.8	.002	.16

TABLE II

Angular vibrational amplitudes for CO on Ru(001), measured with respect to the surface normal.

T	α_o (experimental)	α_i (a) (corrected)	α_{IS} (b) (theory)
90 K	12°	10.8°	10.4°
300 K	16°	14.5°	13.9°

(a) α_i is the experimental value of O^+ hwhm (α_o) after application of the image potential correction (Eq. 1).

(b) α_{IS} is the initial state contribution to the bending vibrational amplitude, based on a model calculation (see text).

FIGURE CAPTIONS

Figure 1 Electron Stimulated Desorption of CO on Ru(001) at $\sim$ 300 K. (a) O^+ ion current as a function of CO exposure; triangles and circles indicate repeat data runs. Electron energy = 210 eV. (b) CO^+ ion current as a function of CO exposure. Electron energy = 210 eV. (c) LEED intensity vs. CO exposure for $\sqrt{3}$ x $\sqrt{3}$ pattern (from Ref. 7).

Figure 2 Retarding potential plots for CO^+ and O^+ in ESD of CO on Ru(001) at $\theta/\theta_{sat} \tilde{-} 0.5$. Electron energy = 150 eV.

Figure 3 Angular distributions of O^+ and CO^+ in ESD of CO on Ru(001). The surface was dosed at 300 K to $\theta/\theta_{sat} \tilde{-} 0.5$, and cooled to 90 K for the measurements. Electron energy = 140 eV.

Figure 4 ESDIAD for O^+ and CO^+ from CO on Ru(001); $\theta/\theta_{sat} \tilde{-} 0.5$. Cone angle α vs crystal bias potential V_B. (a) O^+ cone angle vs. V_B for 300 K and 90 K; (b) CO^+ cone angle vs. V_B for 300 K and 90 K. Points are experimental data; solid lines are based on classical trajectory calculations (see text).

Figure 5 ESDIAD for O^+ and CO^+ from CO on oxygen (2 x 2) layer on Ru(001) at 300 K. Points are experimental data; lines are based on classical trajectory calculations. Solid lines are estimated "best fits"; dashed lines demonstrate effect of varying parameters in classical trajectory calculations.

ELECTRON STIMULATED DESORPTION OF CO ON Ru (001) AT ~300 K

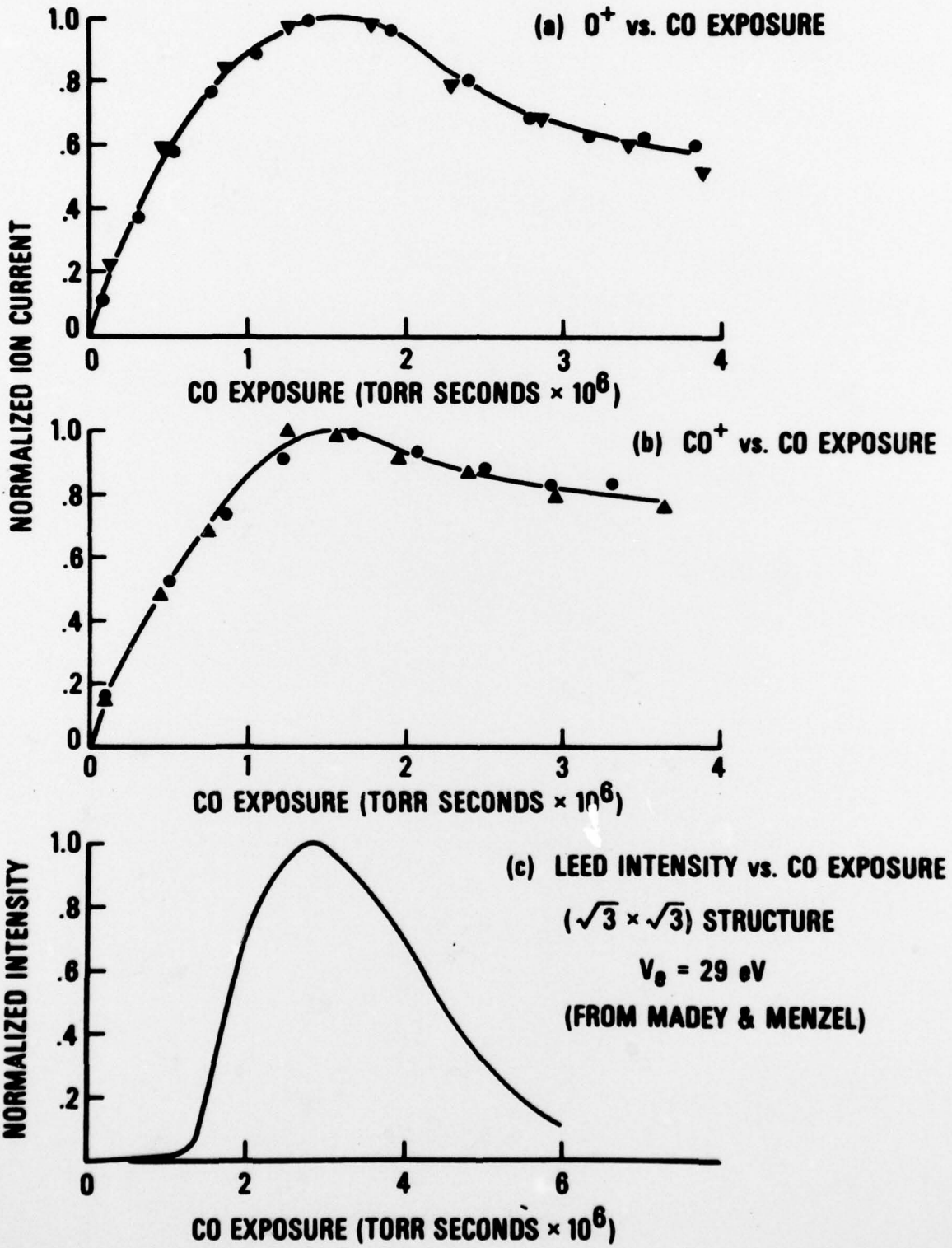

ANGULAR DISTRIBUTIONS OF O^+ AND CO^+ IN ESD OF CO ON Ru (001) AT 90 K

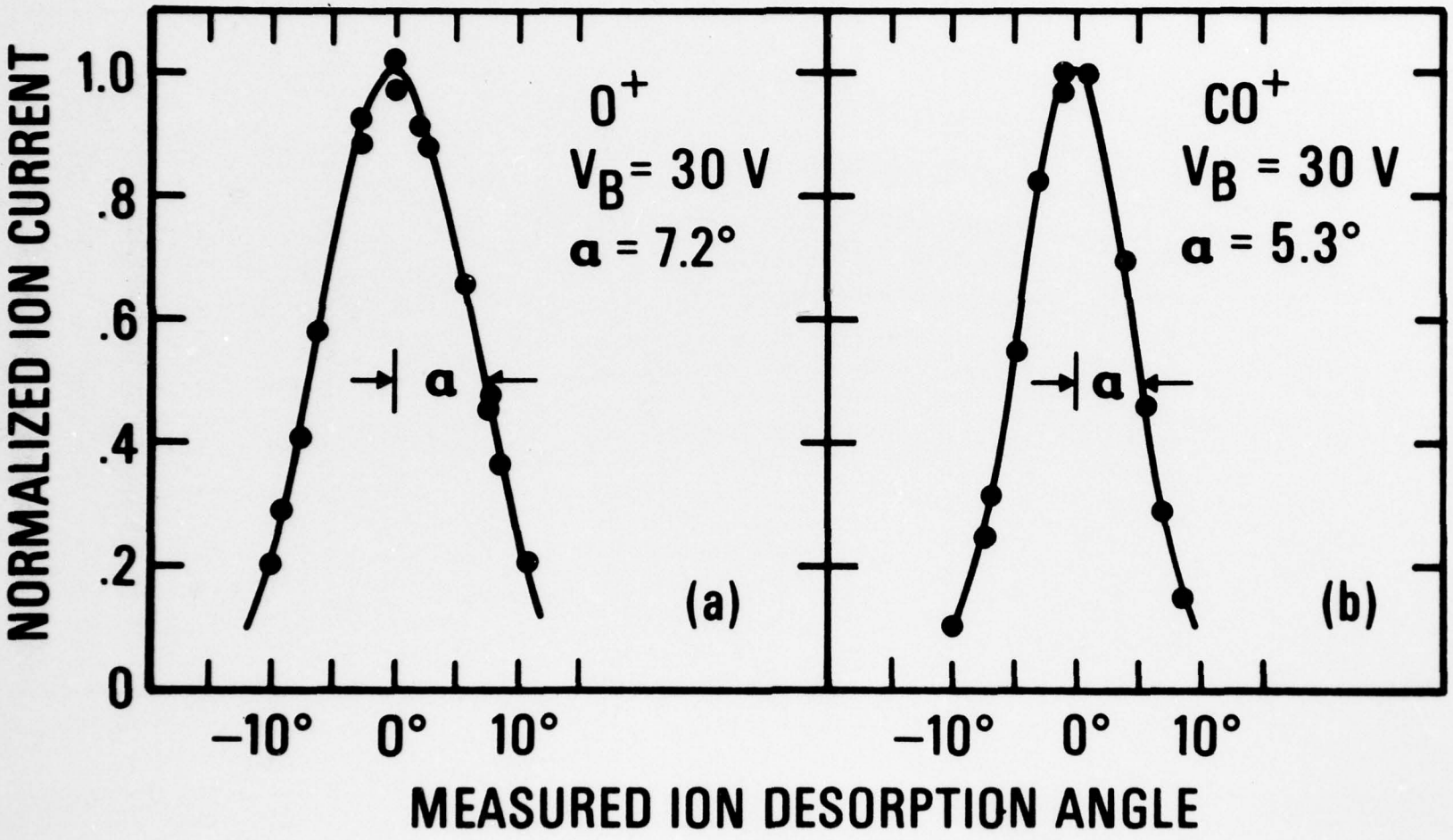

RETARDING POTENTIAL PLOTS FOR CO^+ AND O^+ IN ESD OF CO ON Ru (001)

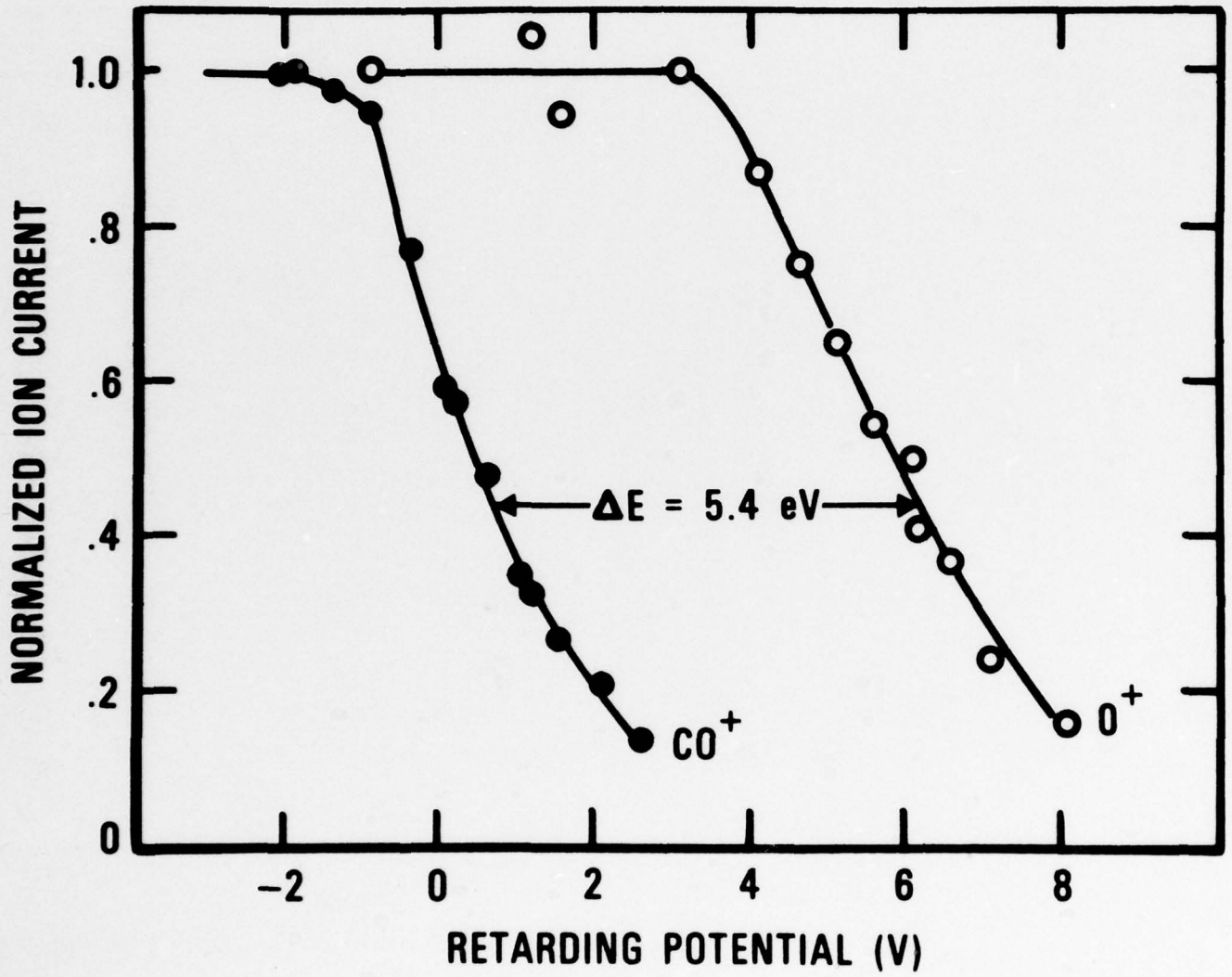

ESDIAD FOR O^+ AND CO^+ FROM CO ON Ru(001); $\theta/\theta_{sat} \simeq 0.5$

CONE ANGLE vs. CRYSTAL BIAS POTENTIAL

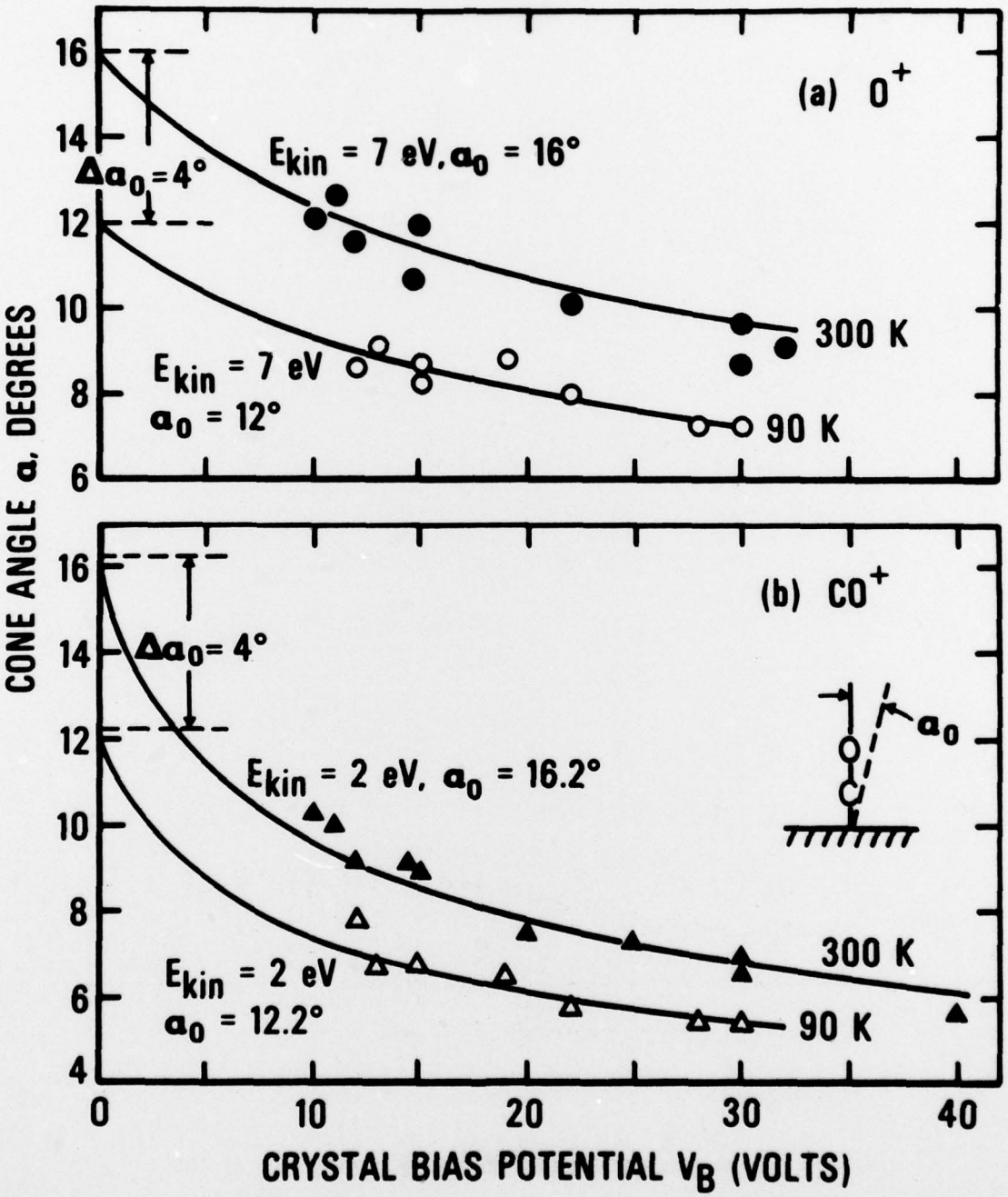

ESDIAD FOR O^+ AND CO^+ FROM CO ADSORBED ON OXYGEN (2x2)/Ru(001) CONE ANGLE vs. CRYSTAL BIAS POTENTIAL